Assessing the effects of subject motion on T 2 relaxation under spin tagging (TRUST) cerebral oxygenation measurements using volume navigators: Effects of Subject Motion on TRUST

HHS Public Access

Author manuscript

Magn Reson Med. Author manuscript; available in PMC 2018 December 01.

Published in final edited form as:

Magn Reson Med. 2017 December ; 78(6): 2283–2289. doi:10.1002/mrm.26616.

Assessing the effects of subject motion on T_2 relaxation under spin tagging (TRUST) cerebral oxygenation measurements using volume navigators

Jeffrey N. Stout[1], **M. Dylan Tisdall**[2,3], **Patrick McDaniel**[4], **Borjan Gagoski**[5], **Divya S. Bolar**[6], **Patricia Ellen Grant**[5,7], and **Elfar Adalsteinsson**[1,4]

[1]Harvard-MIT Health Sciences and Technology, Institute for Medical Engineering & Science, MIT, Cambridge, MA, United States

[2]Athinoula A. Martinos Center for Biomedical Imaging, Massachusetts General Hospital, Charlestown, MA, United States

[3]Radiology, Harvard Medical School, Boston, MA, United States

[4]Department of Electrical Engineering and Computer Science, MIT, Cambridge, MA, United States

[5]Department of Radiology, Boston Children's Hospital, Boston MA, United States

[6]Department of Radiology, Massachusetts General Hospital, Boston, MA, United States

[7]Department of Pediatrics, Boston Children's Hospital, Boston MA, United States

Abstract

Purpose—Subject motion may cause errors in estimates of blood T_2 when using the T_2-relaxation under spin tagging (TRUST) technique on non-compliant subjects like neonates. By incorporating three-dimensional volume navigators (vNavs) into the TRUST pulse sequence, independent measurements of motion during scanning permit evaluation of these errors.

Methods—The effects of integrated vNavs on TRUST-based T_2 estimates were evaluated using simulations and in vivo subject data. Two subjects were scanned with the TRUST+vNav sequence during prescribed movements. Mean motion scores were derived from vNavs and TRUST images, along with a metric of exponential fit quality. Regression analysis was performed between T_2 estimates and mean motion scores. Also, motion scores were determined from independent neonatal scans.

Results—vNavs negligibly affected venous blood T_2 estimates and better detected subject motion than fit quality metrics. Regression analysis showed that T_2 is biased upwards by 4.1 ms per 1 mm of mean motion score. During neonatal scans, mean motion scores of 0.6–2.0 mm were detected.

CORRESPONDING AUTHOR: Jeffrey N. Stout, jstout@mit.edu, (857) 919-1422, 77 Massachusetts Ave, Bldg 36-776A, Cambridge, MA 02139.

SUPPORTING MATERIAL

Supporting Table S1: T_2 estimation and fit quality changes due to the vNav module.

Supporting Figure S1: Empirical signal attenuation due to vNavs

Conclusion—Motion during TRUST causes an overestimate of T_2, which suggests a cautious approach when comparing TRUST-based cerebral oxygenation measurements of noncompliant subjects.

Keywords

TRUST; T_2 relaxation; blood oxygen saturation; motion; volume navigators

INTRODUCTION

A variety of quantitative measures derived from MRI have been found to demonstrate significant biases due to even small amounts of subject motion (1–5), and motion is known to cause high failure rates for MRI studies in non-compliant subjects (6–8). T_2 relaxation under spin tagging (TRUST) is a quantitative technique used to measure cerebral oxygenation (9,10), which is of particular interest in neonates (11–15), but subject motion is prevalent in this cohort. 17% of scans in a previous study of neonates using TRUST were unusable due to motion artifacts (8), and this rate has been as high as 30% in our own investigations (16). Biases due to motion may confound comparisons of cerebral oxygenation measurements between studies.

Similar to many quantitative measures derived from MRI, TRUST relies on comparing changes between image volumes acquired in different experimental conditions. In particular, TRUST uses spin tagging to isolate the venous blood signal in large draining veins of the brain via label and control image subtraction (9). This blood signal is then imaged with varying amounts of T_2 weighting and then fitted with an exponential function to estimate the T_2 relaxation rate of blood. The T_2 of blood is empirically related to its oxygen saturation (17–20). Motion occurring between these two images would presumably affect the venous blood T_2 estimation.

Previous work to assess motion confounds of the TRUST technique was limited to small motions that occurred in otherwise compliant subjects (9,21). This level of evaluation makes sense for compliant subjects considering that two dimensional (2D) registration during data processing would only account for in-plane movements (9,21,22). In relatively still subjects, a correlation between more subject motion and worse exponential fit quality was confirmed, but no statistically significant effect of motion on T_2 or venous oxygen saturation (SvO_2) was reported (9,21). These conclusions cannot be extrapolated to cases where subject motion is large or frequent.

Volume navigators (vNavs) were developed as a means to detect low-frequency subject motion during a scan by using the three-dimensional (3D) imaging capability of the MRI scanner itself (23,24). vNavs are 3D-encoded echo planar images with low resolution, typically $8 \times 8 \times 8$ mm^3, that can be acquired in under 300 ms. vNavs are inserted into a parent sequence during dead-time where magnetization recovery or flow is taking place. Despite the low spatial resolution, sub-millimeter rigid body motions in three dimensions are quantifiable (23,25).

Though vNavs were developed for prospective motion correction, here we used them as a retrospective tool to track subject motion during the TRUST sequence and we evaluated the effects of motion on the estimates of blood T_2. It is extremely difficult to evaluate the effects of motion in the neonatal and infant cohort itself. Anesthesia or sedation that creates a quiescent state may also affect baseline physiology (26–29), and limited scan time for these subjects makes it unlikely that matched baseline no motion and motion corrupted scans can be acquired in the same session. For these reasons, we attempted an initial characterization of the effects of motion on TRUST using healthy adult volunteers. We demonstrated the negligible impact of vNavs on the TRUST-based quantification of T_2 in still subjects, before quantifying the effect of subject motion on T_2 estimates. Finally, we used motion tracks gathered during structural brain scans of neonates to approximate the impact of neonatal motion on TRUST results.

METHODS

TRUST Sequence Modification

We implemented the TRUST sequence (Figure 1A) following the published pulse sequence description (9). Two changes were made: we used adiabatic refocusing pulses in the T_2-preparation module, and we inserted vNav modules before the T_2-preparation module.

The T_2 preparation module consisted of a +90-degree pulse, pairs of hyperbolic secant modulated adiabatic refocusing pulses, and a −90-degree pulse. Inter-echo spacing was 10 ms, such that effective echo times ($TE_{EFFECTIVE}$) of 0, 18, 36, 72 and 144 ms could be generated. The method for determining the correction applied to $TE_{EFFECTIVE}$ due to the duration of the adiabatic pulses and the performance of these pulses has been reported previously (30,31).

vNav acquisition modules (23), consisting of a low resolution 3D-EPI volume acquisition, were inserted into the TRUST sequence. The module was placed directly before the T_2-preparation module, and thus ends at TI - $TE_{EFFECTIVE}$ after the inversion pulse. It was inserted here to be close to the TRUST readout, and so that consistent contrast in the vNavs was maintained between $TE_{EFFECTIVE}$. vNav imaging parameters were: TE/TR = 5.2/11 ms, flip angle = 3°, resolution = 8 × 8 × 8 mm^3, field of view = 256 mm, 6/8 partial Fourier, bandwidth = 4464 Hz/Px, EPI factor = 32, total acquisition time = 300 ms. To test our hypothesis that vNav modules would have negligible effects on the TRUST image magnetization in the absence of subject motion, Bloch simulations of the vNav module were performed (32).

Experiments

All scans of adult subjects took place at the Athinoula A. Martinos Imaging Center at the McGovern Institute for Brain Research, MA, USA. Four adults (2 male, 2 female, mean age=21) were scanned with IRB approval on a Siemens Tim Trio 3T scanner (Siemens Healthineers, Erlangen, Germany) using the Siemens 32-channel head coil. The TRUST image was positioned by visual inspection of a 1 mm^3 isotropic gradient echo structural scan, 25 mm above the confluence of the sinuses perpendicular to the superior sagittal sinus

(SSS). The matrix size was selected to be the same as that used in neonatal imaging so that the number of voxels across the SSS would be similar, but the field of view was 240 mm (160 mm, for neonates). TRUST imaging parameters were: TE/TR = 12/5000 ms, $TE_{EFFECTIVE}$ = 0, 18, 36, 72, 144 ms, resolution = 3.4 × 3.4 × 5 mm^3, inversion time = 1200 ms, tagging width = 100 mm, tagging gap = 25 mm, 3 sets for averaging, total acquisition = 2:30.

TRUST can be used to determine SvO_2 by relating T_2 to saturation via an empirical relationship (17,19,20,33,34). We quantified the effects motion on T_2 estimates, since this relationship is complicated and depends on blood hematocrit and possibly the types of hemoglobin—adult or fetal—present in the blood (33,34).

Each TRUST trial was analyzed using custom Matlab (MathWorks, Natick, MA) routines. The three brightest voxels in a manually drawn ROI of approximately 25 voxels near the SSS were averaged to give a signal intensity ($S(TE_{EFFECTIVE})$) value for one post-subtraction image. Fitting to $S(TE_{EFFECTIVE})=S_0 exp(TE_{EFFECTIVE} *C)$ was performed by taking $ln(S(TE_{EFFECTIVE}))$ and performing a linear least squares fit. The T_2 of blood was then determined as $T_{2,blood}=1/(R_{1,blood}-C)$, $R_{1,blood}=0.62$ (9). Goodness of fit was measured by the standard deviation of the residuals (SDR) of the linear fit.

Empirical test of vNav module's effects—Alternating TRUST and TRUST+vNav trials were gathered from two subjects who were instructed to remain still during the scan, to test the effects of vNav modules on T_2 quantification.

Evaluating the effects of motion on TRUST—To evaluate the effects of motion, two compliant adult subjects were instructed to move their head in a prescribed manner or remain still for alternating TRUST+vNav trials. Motion was rehearsed before entering the scanner for the types, magnitudes and timings of movement given in Table 1. These different motion descriptions were to guarantee a variety of movements, not to validate the accuracy of vNavs nor specify every possible movement. The movement magnitudes were roughly calibrated using the nose bridge on the 32-channel head coil as a guide by asking the subject to move their nose to different positions relative to the nose bridge from the center line (see descriptions in Table 1). Large, medium and small motions equated to a nose movement of approximately 35 mm, 17 and 10 mm respectively with the exact size depending on the facial geometry of the subject. The timing of movements was left up the subjects and so was unknown with respect to sequence timing, but instructions were given to move continuously or re-position with rests between movements.

To accommodate the spin history shadow from the label pulse (Figure 1A), offline registration of the vNav images was performed using the FSL FLIRT tool (35) and custom Matlab scripts. We adapted the methods proposed in (36) to co-register volumes from a region of interest excluding the spin history shadow. Rigid, six degree of freedom, affine translations between each vNav and the first vNav ($T_{1,N}$) were generated. Translations between label and control image pairs were calculated using $T_{L,C} = T_{1,C} (T_{1,L})^{-1}$.

We defined a motion score to reflect movement in the volume near the SSS, reasoning that this motion is what adversely affects blood signal isolation via spin tagging. We adapted the root mean square deviation framework proposed by Jenkinson (37), by setting the volume of interest (VOI) to be a sphere centered on SSS with a 16 mm radius. Thus the motion score for each label and control image pair was:

$$E_{RMS}=\sqrt{\frac{1}{5}R^2\mathrm{Trace}(A^TA)+(t+Ax_c)^T(t+Ax_c)}, \text{where } M=I-T_{L,C}=\begin{bmatrix} A & t \\ 000 & 0 \end{bmatrix}, \quad [1]$$

R = 16 mm, and x_c = center voxel in the SSS. Mean E_{RMS} were calculated for each trial.

For comparison, two dimensional (2D) rigid registrations were performed between label and control TRUST images using FLIRT with the mutual information cost function.

Neonatal motion estimation—To estimate the potential effect of neonatal motion on T_2 estimation, without facing the previously discussed obstacles to performing experiments on neonates, we calculated motion trajectories from vNav data obtained from structural neonatal brain scans gathered as part of another study that took place with IRB approval at Boston Children's Hospital. vNavs from five prospective motion corrected MEMPRAGE scans (Siemens WIP 711), acquired with a Siemens Tim Trio 3T scanner using a 32-channel head coil, were examined to select 2.5 minute periods of motion that had occurred during scanning. The E_{RMS} for movements between TRs was determined using the same methods described previously for our adult study.

RESULTS

TRUST Sequence Modification and Empirical test of vNav module's effects

Bloch simulations of the non-selective, 3° flip angle vNav excitations produced very little attenuation in the difference signal, resulting in a negligible (0.003%) relative decrease in estimated T_2 value of blood. The empirical ratio of TRUST+vNav post-subtraction signal to the TRUST signal was 95.6% (Supporting Figure S1). There were no statistically significant differences in T_2 estimates from the two sequences (Supporting Table S1).

Evaluating the effects of motion on TRUST

Label to control relative motion trajectories for a voxel near the SSS during one moving TRUST scan as measured by the vNav modules (3D) and from TRUST images (2D) are shown in Figure 2.

For 32 TRUST trials, from subjects 3 and 4, where the subject was asked to remain still or to move, mean E_{RMS} and SDR are compared as motion classifiers based on maximum a posteriori probability. The error probability identifying motion trials given mean E_{RMS} was 0.06, and with SDR was 0.17.

The effect of motion on T_2 estimation is shown in Figure 3 and Table 2. Table 2 gives the descriptive statistics for T_2, SDR and mean motion score between label and control images

for alternating motion/still trials. In Figure 3, the T_2 error (difference of T_2 and mean T_2 for still trials) is plotted so that data from two subjects can be combined even though they have different baseline T_2. T_2 error is significantly correlated with E_{RMS} ($R^2 = 0.33$, $P = 0.0005$).

Neonatal motion estimation—The range of mean E_{RMS} motion scores during three periods of motion in neonatal scans was 0.6–2.0 mm. The range of T_2 overestimate predicted from the linear fit was 1.7–7.4 ms. Assuming an actual T_2 of 60 ms, a 7.4 ms overestimation of T_2 would result in an absolute 3.9% bias in SvO_2 (Hct = 0.4, tCPMG = 10 ms) (17,38). Overestimation of SvO_2 with all other factors equal would lead to an underestimation in oxygen extraction fraction and cerebral metabolic rate of oxygen consumption.

DISCUSSION

vNav modules were used to quantify head motion in young adults during TRUST scans. Our main finding is that motion leads to a positive bias in T_2 estimates (4.1 ms per mm of mean E_{RMS}), as well as increased variance. This bias could be as large as half of the physiological change some studies have tried to detect. In addition, we found that motion detection using vNavs was a more accurate classifier than relying on quality of T_2 fit. These findings are important because when the TRUST technique is used in studies with poor patient compliance to instructions to remain still (8), or in cohorts with different propensities to motion, due to disease or anesthesia (16), the bias introduced by motion should be considered when drawing conclusions about brain state in these different groups. A conundrum results, because obvious methods to mitigate motion, like sedation, anesthesia or restraint may all alter the baseline $CMRO_2$ being quantified (26–29) and it is generally impossible to sedate or anesthetize healthy controls for still comparison between brain states.

There are a few caveats pertaining to the approximate T_2 bias of 1.7–7.4 ms due to neonatal motion. vNavs were acquired every 2.52 seconds in the MEMPRAGE scans so the motion tracks provide a lower bound on the TRUST mean E_{RMS} (TR = 5 seconds) since subjects would have more time to move between the label and control images in the TRUST sequence. Also, though we tried to mimic the partial volume effects expected in neonates by matching image matrix sizes between adult and neonatal scans, there is a fundamental difference in signal to noise ratio in the different voxel sizes. We expect this difference to affect the variance rather than the bias of the T_2 estimate. Lastly, neonates may move differently than the adult motions we prescribed.

Despite these caveats, a 7.4 ms bias in T_2 is important since it exceeds the largest same subject standard deviation (SD) in T_2 observed in this study (3.9 ms, Table 2) and the mean same subject SD given in a study investigating the test-retest characteristics of TRUST (4.5 ms, backed out from the SvO_2 results in (39) by assuming a hematocrit of 0.4, SvO_2 of 62% (39), and a τ_{CPMG} of 10 ms). Potential bias due to motion alone (3.9% absolute SO_2) is greater than half the observed group difference in SvO_2 in some studies of neonates with congenital heart disease (7.5% absolute SO_2) (40).

Motion leads to increased measurement variance in addition to a positive bias as seen in Table 2 and Figure 3. Our observed average intrasession (same subject measurements from one session) SD for motion trials (8.4 ms) shows that motion adds significant measurement uncertainty—of a comparable magnitude to the observed *intersubject* SD for still trials (6.0 ms)—to the T_2 estimate in addition to the upward bias. This is further evidence that motion may confound intersubject comparisons. The intrasession and intersubject SD (Table 2) for still trials are similar to the values previously reported by the TRUST developers (9,39). Still trial intrasession variance is due to measurement and physiological noise. The additional variance with motion not explained by mean E_{RMS} could be due to motion affecting only some label-control pairs, or motion could be sufficiently severe to affect the volume of the cortex that is labeled by the inversion affecting the overall signal to noise ratio of the technique.

To explore how motion may affect the underlying TRUST signal, the equations in (9) can be modified to include a change (Δ) in blood volume fraction in a voxel (X_b) between the control and label acquisitions, where $0 \leq X_b \leq 1$ and $X_b\text{-}1 \leq \Delta \leq X_b$.

$$\Delta S = X_b S_{\text{blood, control}} - \Delta S_{\text{tissue}} - (X_b - \Delta) S_{\text{blood, label}} \quad [2]$$

Lumping terms that do not depend on $TE_{EFFECTIVE}$ (subscript b, blood, and t for tissue):

$$\Delta S = S_1(X_b - \Delta) e^{TE_{EFF}(\frac{1}{T_{1,b}} - \frac{1}{T_{2,b}})} + S_2(\Delta) e^{\frac{-TE_{EFF}}{T_{2,b}}} - S_3(\Delta) e^{\frac{-TE_{EFF}}{T_{2,t}}} + S_4(\Delta) e^{TE_{EFF}(\frac{1}{T_{1,t}} - \frac{1}{T_{2,t}})}$$

[3]

Considering that for moving subjects data is gathered with different Δ values for each $TE_{EFFECTIVE}$, and that this will lead to different weighting of the exponentials, it is unsurprising that much of the final variance in T_2 is unexplained by mean E_{RMS}.

The derivation of Equation 3 assumes no motion during the readout and no velocity effects causing additional signal modulation. Higher frequency motion tracking, perhaps obtained via optical methods (41), could be used to explore these effects. However, given our observations, further work on motion correction for TRUST should adopt a detect and reject strategy using volume navigators, or perform prospective motion correction for all label, saturation, preparation and readout pulses using a sequence-independent motion tracking system.

To assess and correct for motion in TRUST, researchers have relied on 2D registration of label and control images, visual inspection of the post-subtraction images, and/or some quality of exponential fit metric (8,9,21,39,42). All these methods rely on the intrinsic information in the 2D TRUST images. This information is incomplete since out of plane motions go undetected as is demonstrated by Figure 2. Figure 3 shows that 3D motion tracks describe more of the variance in T_2 error than do 2D motion tracks (R^2 = 0.27 versus 0.33).

Against the vNav benchmark, Figure 3 shows that the 2D mean E_{RMS} metric actually captures the majority of the variance in T_2 error. This might be due to the basically perpendicular orientation of the SSS with respect to the imaging plane, and suggests motion tracks derived from previously acquired data sets could be used to inform intersubject or group-wise comparisons of SvO_2.

We did not implement the suggested pulse sequence upgrades in (22), but we do not expect either improvement to affect our conclusions. Areas of the brain may be in a different metabolic states between motion and still trials, but previous studies suggest this is negligible for global measurements (43,44).

In conclusion, vNavs used to monitor 3D motion during TRUST show that motion causes an overestimate of T_2, and this bias may affect SvO_2 estimates in non-compliant subjects such as infants or neonates.

Supplementary Material

Refer to Web version on PubMed Central for supplementary material.

Acknowledgments

This publication was made possible by NIBIB-NIH grants 5T32EB1680, R01EB017337, U01HD087211, by NIH-NICHD grants 4R00HD074649-03, R21HD072505. Scans were carried out at the Athinoula A. Martinos Imaging Center at the McGovern Institute for Brain Research, MIT.

REFERENCES

1. Reuter M, Tisdall MD, Qureshi A, Buckner RL, van der Kouwe AJW, Fischl B. Head motion during MRI acquisition reduces gray matter volume and thickness estimates. Neuroimage [Internet]. 2015; 107:107–115.
2. Yendiki A, Koldewyn K, Kakunoori S, Kanwisher N, Fischl B. Spurious group differences due to head motion in a diffusion MRI study. Neuroimage [Internet]. 2014; 88:79–90.
3. Van Dijk KRA, Sabuncu MR, Buckner RL. The influence of head motion on intrinsic functional connectivity MRI. Neuroimage [Internet]. 2012; 59:431–438.
4. Power JD, Barnes KA, Snyder AZ, Schlaggar BL, Petersen SE. Spurious but systematic correlations in functional connectivity MRI networks arise from subject motion. Neuroimage [Internet]. 2012; 59:2142–2154.
5. Satterthwaite TD, Wolf DH, Loughead J, Ruparel K, Elliott MA, Hakonarson H, Gur RC, Gur RE. Impact of in-scanner head motion on multiple measures of functional connectivity: Relevance for studies of neurodevelopment in youth. Neuroimage [Internet]. 2012; 60:623–632.
6. Yerys BE, Jankowski KF, Shook D, Rosenberger LR, Barnes A, Berl MM, Ritzl EK, Vanmeter J, Vaidya CJ, Gaillard WD. The fMRI success rate of children and adolescents: typical development, epilepsy, attention deficit/hyperactivity disorder, and autism spectrum disorders. Hum. Brain Mapp. 2010; 30:3426–3435.
7. Dylan Tisdall M, Reuter M, Qureshi A, Buckner RL, Fischl B, van der Kouwe AJW. Prospective motion correction with volumetric navigators (vNavs) reduces the bias and variance in brain morphometry induced by subject motion. Neuroimage [Internet]. 2015; 127:11–22.
8. Liu P, Huang H, Rollins N, Chalak LF, Jeon T, Halovanic C, Lu H. Quantitative assessment of global cerebral metabolic rate of oxygen (CMRO2) in neonates using MRI. NMR Biomed. [Internet]. 2014
9. Lu H, Ge Y. Quantitative evaluation of oxygenation in venous vessels using T2-Relaxation-Under-Spin-Tagging MRI. Magn. Reson. Med. [Internet]. 2008; 60:357–363.

10. Xu F, Ge Y, Lu H. Noninvasive quantification of whole-brain cerebral metabolic rate of oxygen (CMRO2) by MRI. Magn. Reson. Med. [Internet]. 2009; 62:141–148.
11. Liu P, Chalak LF, Lu H. Non-invasive assessment of neonatal brain oxygen metabolism: A review of newly available techniques. Early Hum. Dev. [Internet]. 2014; 90:695–701.
12. Limperopoulos C, Tworetzky W, McElhinney DB, et al. Brain volume and metabolism in fetuses with congenital heart disease: evaluation with quantitative magnetic resonance imaging and spectroscopy. Circulation [Internet]. 2010; 121:26–33.
13. Sun L, Macgowan CK, Sled JG, et al. Reduced Fetal Cerebral Oxygen Consumption Is Associated With Smaller Brain Size in Fetuses With Congenital Heart Disease. Circulation [Internet]. 2015; 131:1313–1323.
14. Jain V, Buckley EM, Licht DJ, et al. Cerebral oxygen metabolism in neonates with congenital heart disease quantified by MRI and optics. J. Cereb. Blood Flow Metab. [Internet]. 2014; 34:380–388.
15. Cheng HH, Wypij D, Laussen PC, Bellinger DC, Stopp CD, Soul JS, Newburger JW, Kussman BD. Cerebral blood flow velocity and neurodevelopmental outcome in infants undergoing surgery for congenital heart disease. Ann. Thorac. Surg. [Internet]. 2014; 98:125–132.
16. Stout, JN., Ferradal, SL., Zollei, L., Bolar, DS., Lin, A., Gagoski, B., Cheng, H., Adalsteinsson, E., Grant, PE. Optimizing unanesthetized cerebral oxygen consumption measures: comparison of MRI and near-infrared spectroscopy (NIRS) approaches in neonates with congenital heart disease. ISMRM Annual Meeting; Singapore. 2016. p. 735
17. Lu H, Xu F, Grgac K, Liu P, Qin Q, van Zijl P. Calibration and validation of TRUST MRI for the estimation of cerebral blood oxygenation. Magn. Reson. Med. [Internet]. 2012; 67:42–49.
18. Wright GA, Hu BS, Macovski A. 1991 I.I. Rabi Award. Estimating oxygen saturation of blood in vivo with MR imaging at 1.5 T. J. Magn. Reson. Imaging [Internet]. 1991; 1:275–283.
19. Zhao JM, Clingman CS, Närväinen MJ, Kauppinen Ra, van Zijl PCM. Oxygenation and hematocrit dependence of transverse relaxation rates of blood at 3T. Magn. Reson. Med. [Internet]. 2007; 58:592–597.
20. Bush A, Borzage M, Detterich J, Kato RM, Meiselman HJ, Coates T, Wood JC. Empirical model of human blood transverse relaxation at 3 T improves MRI T_2 oximetry. Magn. Reson. Med. [Internet]. 2016; 0:1–8.
21. Liu P, Dimitrov I, Andrews T, et al. Multisite evaluations of a T2 -relaxation-under-spin-tagging (TRUST) MRI technique to measure brain oxygenation. Magn. Reson. Med. [Internet]. 2016; 75:680–687.
22. Xu F, Uh J, Liu P, Lu H. On improving the speed and reliability of T2-relaxation-under-spin-tagging (TRUST) MRI. Magn. Reson. Med. [Internet]. 2012; 68:198–204.
23. Tisdall MD, Hess AT, Reuter M, Meintjes EM, Fischl B, van der Kouwe AJW. Volumetric navigators for prospective motion correction and selective reacquisition in neuroanatomical MRI. Magn. Reson. Med. [Internet]. 2012; 68:389–399.
24. Hess AT, Tisdall MD, Andronesi OC, Meintjes EM, van der Kouwe AJW. Real-time motion and B0 corrected single voxel spectroscopy using volumetric navigators. Magn. Reson. Med. [Internet]. 2011; 66:314–323.
25. Zhang, Y., Aganj, I., Kouwe, JW Van Der, Tisdall, MD. Effects of Resolution and Registration Algorithm on the Accuracy of EPI vNavs for Real Time Head Motion Correction in MRI; Proceedings of the IEEE Conference on Computer Vision and Pattern Recognition Workshops; 2016. p. 143-151.
26. Carlsson C, Smith DS, Keykhah MM, Englebach I, Harp JR. The effects of high-dose fentanyl on cerebral circulation and metabolism in rats. Anesthesiology [Internet]. 1982; 57:375–380.
27. LN M, Milde JH, WJ G. Cerebral effects of fentanyl in dogs. Br. J. Anaesth. 1989:710–715. [PubMed: 2514778]
28. Uematsu M, Takasawa M, Hosoi R, Inoue O. Uncoupling of flow and metabolism by chloral hydrate: a rat in-vivo autoradiographic study. Neuroreport [Internet]. 2009; 20:219–222.
29. Lynch, JM., Ko, T., Newland, JJ., Winters, M., Buech, DR., Nicolson, SC., Montenegro, LM., Yodh, AG., Licht, DJ. Effect of anesthesia on cerebral oxygenationand blood flow in neonates with critical congenital heart disease; OSA Biomedical Optics Congress; 2016.

30. Bolar DS. Magnetic Resonance Imaging of the Cerebral Metabolic Rate of Oxygen Consumption (CMRO2). Massachusetts Institute of Technology. 2010

31. Bolar DS, Rosen BR, Sorensen AG, Adalsteinsson E. QUantitative Imaging of eXtraction of Oxygen and TIssue Consumption (QUIXOTIC) Using Venular-Targeted Velocity- Selective Spin Labeling. Magn. Reson. Med. [Internet]. 2011; 66:1550–1562.

32. Hargreaves B. Bloch Equation Simulator. 2003

33. Liu P, Chalak LF, Krishnamurthy LC, Mir I, Peng S, Huang H, Lu H. T1 and T2 values of human neonatal blood at 3 Tesla: Dependence on hematocrit, oxygenation, and temperature. Magn. Reson. Med. [Internet]. 2015; 0 n/a-n/a.

34. Portnoy, S., Seed, M., Zhu, J., Sled, J., Macgowan, C. Combined T 1 and T 2 Measurement for Non-Invasive Evaluation of Blood Oxygen Saturation and Hematocrit Methods. Vol. 39. Toronto, Canada: ISMRM; 2015. p. 129

35. Jenkinson M, Bannister P, Brady M, Smith S. Improved optimization for the robust and accurate linear registration and motion correction of brain images. Neuroimage. 2002; 17:825–841. [PubMed: 12377157]

36. McDaniel P, Gagoski B, Tisdall MD, van der Kouwe AJW, Grant PE, Wald LL, Adalsteinsson E. Quantification of Fetal Motion Tracked with Volumetric Navigator MRI Acquisitions. Proc. Intl. Soc. Mag. Reson. 2015

37. Jenkinson M. Measuring Transformation Error by RMS Deviation. FMRIB Tech. Rep. TR99MJ1. 2012

38. Jopling J, Henry E, Wiedmeier SE, Christensen RD. Reference ranges for hematocrit and blood hemoglobin concentration during the neonatal period: data from a multihospital health care system. Pediatrics. 2009; 123:e333–e337. [PubMed: 19171584]

39. Liu P, Xu F, Lu H. Test-retest reproducibility of a rapid method to measure brain oxygen metabolism. Magn. Reson. Med. [Internet]. 2013; 69:675–681.

40. Dehaes M, Cheng HH, Buckley EM, et al. Perioperative cerebral hemodynamics and oxygen metabolism in neonates with single-ventricle physiology. Biomed. Opt. Express [Internet]. 2015; 6:4749.

41. Maclaren J, Herbst M, Speck O, Zaitsev M. Prospective motion correction in brain imaging: a review. Magn. Reson. Med. [Internet]. 2013; 69:621–636.

42. Rodgers ZB, Englund EK, Langham MC, Magland JF, Wehrli FW. Rapid T2- and susceptometry-based CMRO2 quantification with interleaved TRUST (iTRUST). Neuroimage [Internet]. 2015; 106:441–450.

43. Vafaee MS, Vang K, Bergersen LH, Gjedde A. Oxygen consumption and blood flow coupling in human motor cortex during intense finger tapping: implication for a role of lactate. J. Cereb. Blood Flow Metab. [Internet]. 2012; 32:1859–1868.

44. Donahue MJ, Blicher JU, Østergaard L, Feinberg Da, MacIntosh BJ, Miller KL, Günther M, Jezzard P. Cerebral blood flow, blood volume, and oxygen metabolism dynamics in human visual and motor cortex as measured by whole-brain multi-modal magnetic resonance imaging. J. Cereb. Blood Flow Metab. 2009; 29:1856–1866. [PubMed: 19654592]

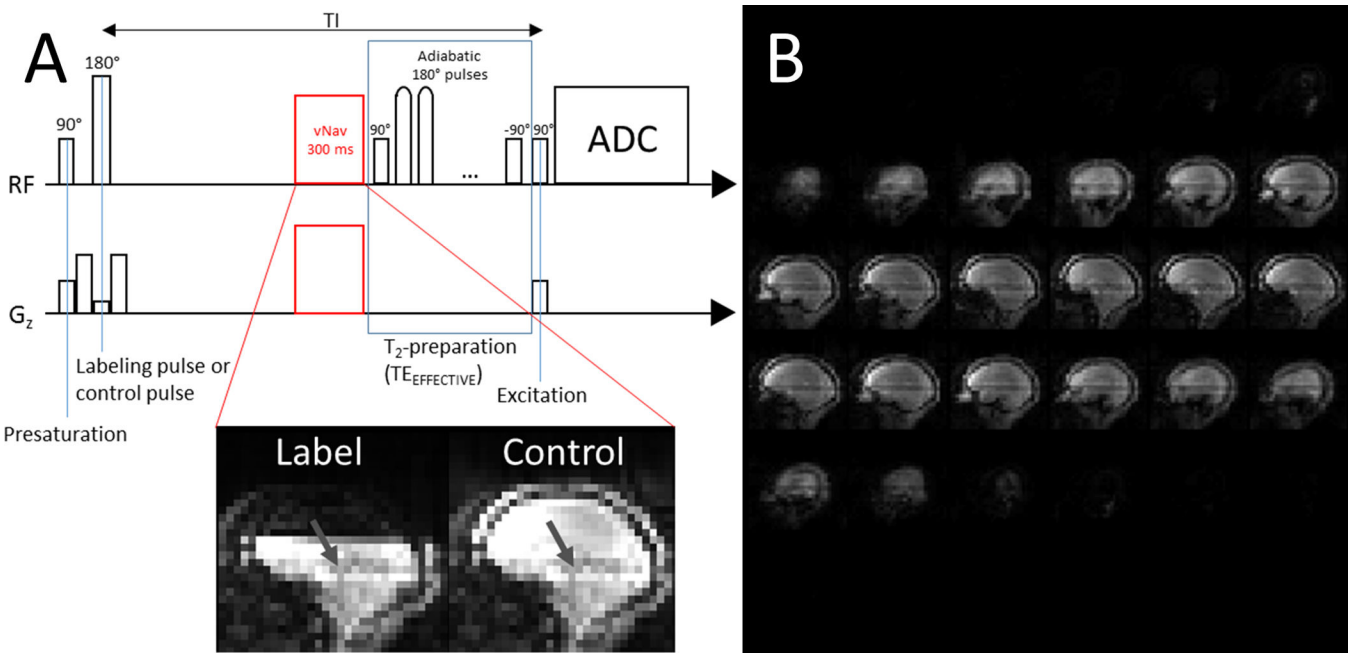

Figure 1.

The TRUST pulse sequence diagram with vNav module (a), with arrows indicating the pre-saturation shadow for the imaging slice. The vNav module begins at different times depending on $TE_{EFFECTIVE}$ (at TI-$TE_{EFFECTIVE}$-300ms after the inversion labeling pulse). Example set of sagittal images from the vNav module acquired during a control acquisition (b).

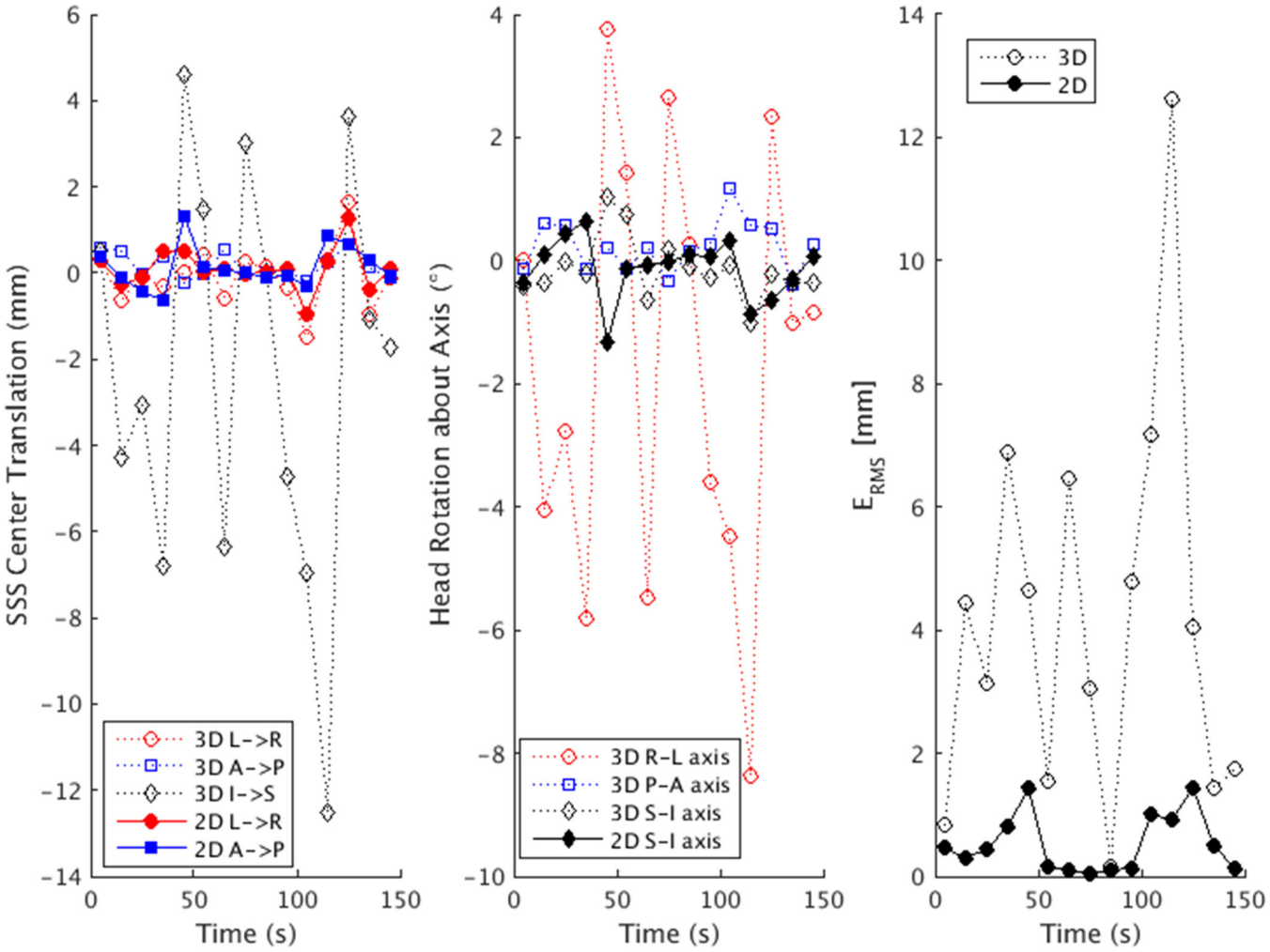

Figure 2.

Example vNav (3D) and TRUST image (2D) derived motion trajectories for one trial where the subject was asked to "nod with large motions continuously." Each point represents the motion between one label-control image pair along the left-right (L-R), A-P (anterior-posterior) and inferior-superior (I-S) axes. (Translations between label and control pairs are defined for a voxel centered on the SSS, and rotations derived from the $T_{L,C}$ matrices.)

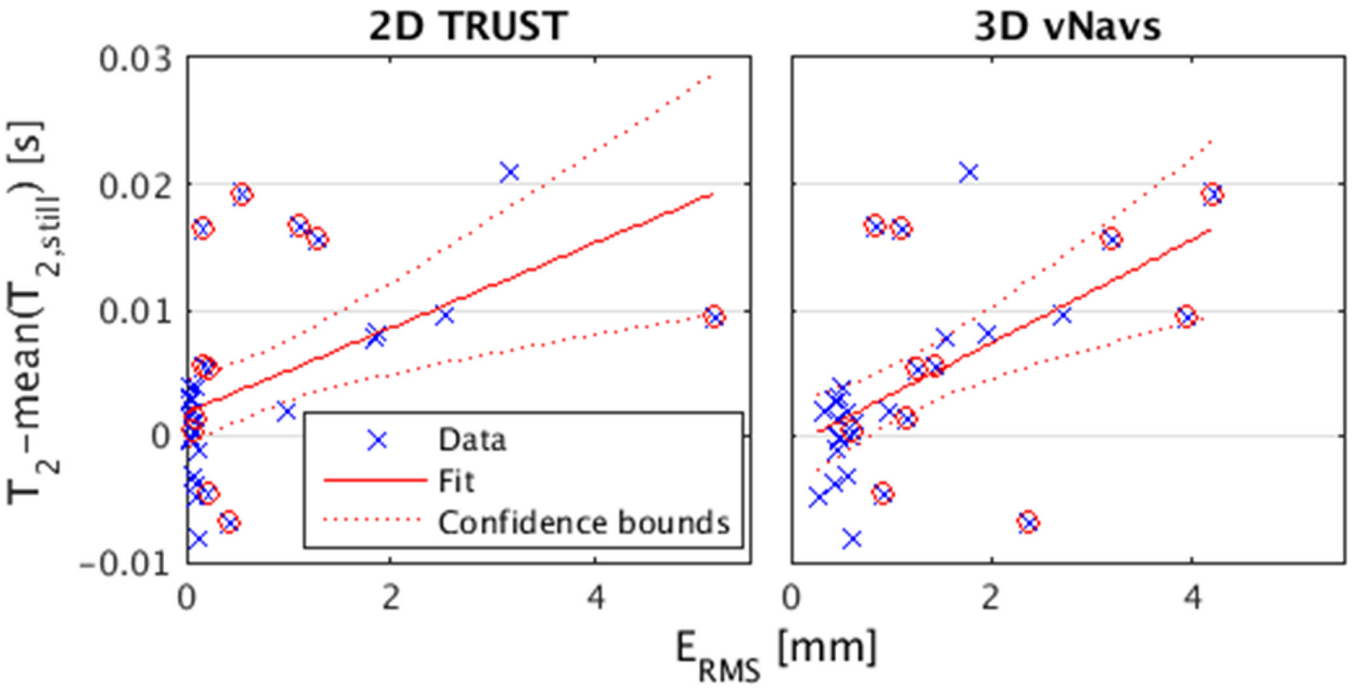

Figure 3.

The difference between T_2 and mean T_2 during all still trials for each subject versus mean E_{RMS} as calculated from 2D TRUST and 3D vNav registrations, respectively. Red circles indicate trials were translations along the inferior-superior axis exceed 1 mm. Linear regression line for TRUST y=0.0034x+0.0018, R^2 = 0.27, P = 0.002 and for vNavs y=0.0041x-0.0008, R^2 = 0.33, P = 0.0005.

Table 1

Prescription for motion, one attribute from each column was selected for each motion trial.

Type of motion	Magnitude of motion	Timing of motion
“yes” nod (rotation about a right-left axis)	Large (move the nose from touching one side of the nose bridge to the other, or similar perceived motion)	Continuously (“slowly move without stopping”)
“no” shake (rotation about an inferior-superior axis)	Medium (move the nose from center to touching on one side nose bridge, or similar perceived motion)	Re-position with rests (“move to a new position and hold it for a couple of breaths, then repeat”)
random (combinations of nodding and rotation as well as translations)	Small (from center to the side without touching the nose bridge, or similar perceived motion)	

Table 2

Mean +/− standard deviation for T_2, SDR and mean motion score for all trials (* indicates $P > 0.05$ for the unpaired T-test between no-motion and motion states)

	No Motion				Motion			
Subject	**N, trials**	**T_2 [ms]**	**SDR**	**mean(E_{RMS}) [mm]**	**N, trials**	**T_2 [ms]**	**SDR**	**mean(E_{RMS}) [mm]**
3	8	60.6 ± 3.9	0.09 ± .02	0.58 ± .08	8	67.0 ± 8.1	0.19 ± .14	2.36 ±1.70*
4	8	51.0 ± 3.0	0.11 ± .02	0.44 ± .09	8	60.5 ± 8.7*	0.26 ± .08*	1.93 ± 0.79*
All	16	55.8 ± 6.0	0.10 ± .03	0.51 ± .11	16	63.8 ± 8.8*	0.22 ± .12*	2.15 ± 1.30*